ARMY RESEARCH LABORATORY

User Manual for the Microsoft Window Edition of the Scanning Fast-Field Program (WSCAFFIP) Version 3.0

by John M. Noble

ARL-TR-2696   January 2003

20030213 038

NOTICES

Disclaimers

Army Research Laboratory
Adelphi, MD 20783-1197

ARL-TR-2696

January 2003

User Manual for the Microsoft Window Edition of the Scanning Fast-Field Program (WSCAFFIP) Version 3.0

John M. Noble
Computational and Information Sciences Directorate, ARL

Contents

List of Figures

List of Tables

1. Introduction

The Scanning Fast-Field Program (SCAFFIP) is based on the Fast-Field Program (FFP) with the added ability to scan multiple frequencies when one is predicting the propagation conditions, about the location of a sensor. SCAFFIP makes a prediction of the acoustic propagation conditions, based on geometrical spreading, molecular absorption, refraction, acoustically complex ground impedance, and diffraction because of refraction over flat terrain. The Microsoft Windows version uses the output of SCAFFIP to build a matrix of sound attenuation versus frequency and range. The attenuation matrix can be used as input to Battlefield or acoustic sensor simulations such as CASTFORM, JANUS, and BASIS.

The FFP is a one-way solution to the acoustic wave equation originally developed for underwater sound propagation predictions [1,2] Raspet et al. [3] and Lee et al. [4] adapted the FFP to propagation in the atmosphere. The FFP developed by Raspet et al. used a propagation matrix formulation. If each layer in the atmosphere is viewed as an optical device, a matrix for each layer in the atmosphere can be constructed. Multiplying each matrix together results in a new matrix that represents how an acoustic signal will be affected as it propagates through the atmosphere. Next, a Bessel Function Transform of the problem is taken with respect to range. After the solution is calculated, an inverse transform is performed to achieve the final solution.

The software package that comes with Microsoft Window Edition of the Scanning Fast-Field Program (WSCAFFIP) is an integrated set of algorithms for running the acoustic propagation model on a PC-based computer platform running Microsoft Windows 95 or higher. Sample test cases (in Appendix A) show the structure of the input files used by WSCAFFIP and give the user a basis to verify their installation. The software package is available on several media, including e-mail. The current version of WSCAFFIP does not contain an installation program, so the user must copy the files to his or her desired directory. A self-extracting archive version is available which assists in copying the files to the correct directory. Section 4.1 gives the step-by-step procedure for installing WSCAFFIP.

2. Propagation Theory

2.1 Speed of Sound

Meteorological phenomena can have a significant effect on the received sound field. Some of the meteorological variables affecting the speed of sound in air are pressure, temperature, wind velocity, and humidity. To observe the effect of each meteorological variable, consider each one

1

independently and examine the equation for the speed of sound in air. The value c, according to Laplace's adiabatic assumption for air as an ideal gas, [5] is

$$c(T) = \sqrt{\frac{gRT}{M}} \qquad (2.1)$$

in which γ is the ratio of specific heats, R is the universal gas constant equal to 8314.16 J/(kg K), and M is the molecular weight of air.

The presence of water molecules alters the sound speed by lowering g and decreasing M. The decreased M dominates so that the overall effect of increasing humidity is an increasing sound speed. These changes can be quantified as

$$\gamma = \frac{7 + h}{5 + h} \qquad (2.2)$$

and

$$M = 29 - 11\,h \qquad (2.3)$$

in which h is the fraction of water molecules in air. As the amount of water in the atmosphere increases, the molecular weight of a parcel of air will decrease since the molecular weight of a water molecule is less than diatomic nitrogen and diatomic oxygen. As a result, the sound speed increases as the fraction of water molecules in the air increases. In order to calculate the fraction of water molecules in air, the *Goff-Gratch equation* must be used to first calculate the partial pressure of saturated water vapor, P_{sat} at temperature T. This equation is

$$\begin{aligned}
\log_{10}\left(\frac{P_{sat}}{P_o}\right) &= 10.79586\left[1 \pm \left(\frac{T_{01}}{T}\right)\right] \pm 5.02808\log_{10}\left(\frac{T}{T_{01}}\right) \\
&+ 1.5047\text{x}10^{-4}\left(1 - 10^{-8.29692[(T/T_{01})-1]}\right) \\
&+ 0.42873\text{x}10^{-3}\left(10^{4.76955[1-(T_{01}/T)]} - 1\right) - 2.2195983
\end{aligned} \qquad (2.4)$$

in which $T_{01} = 273.16$ K and $p_o = 1$ atm or the reference pressure.

After the value for P_{sat} is determined, the fraction of water molecules in air can be calculated by the following relationship:

$$h = \frac{10^{-2}(RH)P_{sat}}{P} \qquad (2.5)$$

in which RH is the relative humidity in percent and P is the pressure in atmospheres.

The magnitude of the dependence of the sound speed on humidity is not obvious. To understand the degree of the effect of humidity on sound speed, consider a particular case. At 20 °C, the difference in sound speed between 0% and 100% humidity is 2 m/s. A fluctuation in the humidity of this amount is very unlikely. If the variation in humidity is reduced to a change of 50% to

100%, the change in the sound speed is only 1 m/s. Therefore, the variation of sound speed caused by changes in humidity should always be much less than 1 m/s. Generally, humidity fluctuations can be ignored.

The effect of the wind speed on the speed of sound is a vector relation. The effective sound speed is calculated by

$$c_{eff} = c(T) + u \times \cos(q_w - p - q_R) \tag{2.6}$$

in which $c(T)$ is the speed of sound in the absence of wind at temperature T, u is the magnitude of the horizontal wind speed, θ_R is the bearing of the receiver from the source, θ_w is the direction from which the wind blows, and $\theta_w - \pi$ is the direction the wind is blowing (see Figure 1). All directions are relative to north.
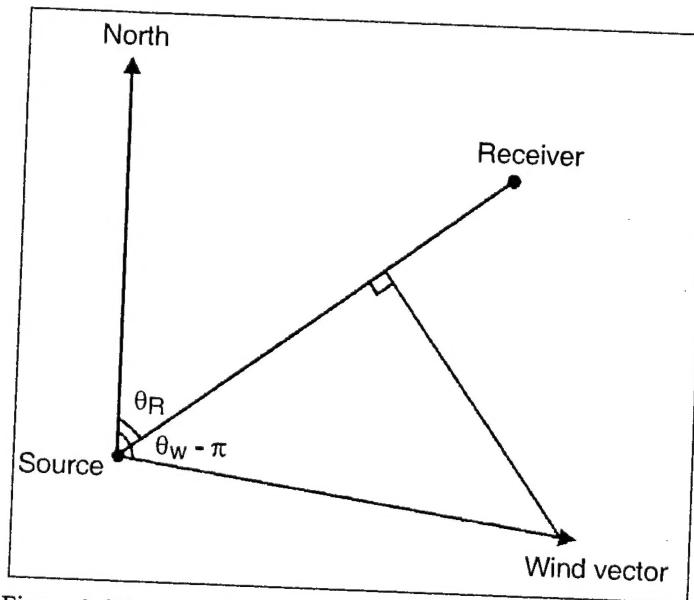
Figure 1. Diagram of geometry definition.

The sound speed will also vary with height because the sound speed is a function of temperature and vector wind speed. This variation will cause the acoustic wave to be refracted as it propagates through the atmosphere. The degree of refraction that the wave undergoes is related to the sound speed gradient present in the atmosphere. If the sound speed increases with height, the acoustic wave will be refracted downward. If the sound speed decreases with height, the acoustic wave will be refracted upward.

2.2   Fast-Field Program (FFP)

The propagation of sound from a point source at the origin is given by the classical wave equation

$$\nabla^2 p - \frac{1}{c^2} \frac{\partial^2 p}{\partial t^2} = -4\pi\delta(x, y, z) \tag{2.7}$$

3

in which δ represents a delta function source of unit strength. For simple harmonic motion, we may replace $\partial/\partial t$ by $-i\omega$, so Equation (2.7) becomes the Helmholtz equation

$$\nabla^2 p - k^2 p = -4p\delta(x,y,z) \qquad (2.8)$$

in which k is the wave number, ω/c, in which c is the sound speed and ω is the angular frequency. For the FFP, c is restricted to vary only in the z-direction.

Transforming Equation (2.8) into cylindrical coordinates and assuming azimuthal symmetry, the Helmholtz equation becomes

$$\frac{\partial^2 p}{\partial r^2} + \frac{1}{r}\frac{\partial p}{\partial r} + p\frac{\partial}{\partial z}\left(\frac{1}{p}\frac{\partial p}{\partial z}\right) + k^2 p = \frac{2}{r}\delta(r)\delta(z - z_s) \qquad (2.9)$$

in which the source is located at $r = 0$ and $z = z_s$ and ρ is the density of the medium.

The atmosphere is viewed as a series of constant sound speed layers for the FFP (as shown in Figure 2). The layers in the atmosphere are bound on top and bottom by complex impedance surfaces. The top boundary is typically modeled as an infinite half-space with constant parameters. At the bottom boundary, the atmospheric layer adjoins a partially absorbing surface within can be represented by the complex acoustical impedance of the ground.
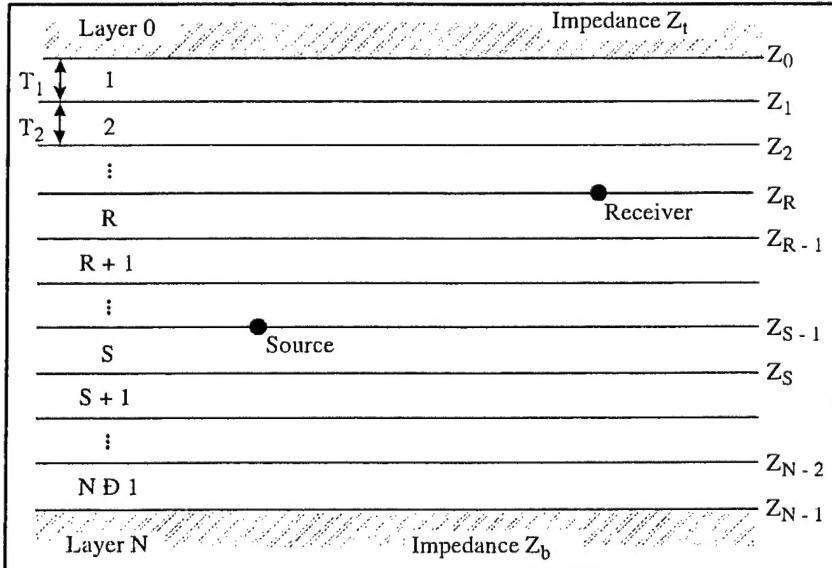
Figure 2. Graphic representation of WSCAFFIP's view of the atmosphere.

To reduce the dimensionality of Equation (2.9), a zero-order Hankel transform is applied with respect to the range variable r. We define the transform pair:

$$\begin{aligned}
\breve{p}(\kappa,z) &= \int_0^\infty p(r,z)J_o(\kappa r)rdr \\
p(r,z) &= \int_0^\infty \breve{p}(\kappa,z)J_o(\kappa r)\kappa d\kappa
\end{aligned} \qquad (2.10)$$

4

Applying the first transform to Equation (2.9) results in

$$\frac{d^2\breve{p}}{dz^2} + \left[k^2(z) - \kappa^2\right]\breve{p} = -2\delta(z - z_s) \quad . \tag{2.11}$$

Since $\rho_o \, \partial u_z / \partial t = \partial p / \partial z$, we now have the following coupled equations:

$$\breve{u}_z = \frac{i}{\omega\rho_o} \frac{d\breve{p}}{dz} \tag{2.12}$$

$$\frac{d\breve{u}_z}{dz} = \frac{i}{\omega\rho_o} \frac{d^2\breve{p}}{dz^2} = -\frac{i}{\omega\rho_o}\left[k^2(z) - \kappa^2\right]\breve{p} + \frac{2}{i\omega\rho_o}\delta(z - z_s) \tag{2.13}$$

in which ρ_o is the mean air density and $\breve{u}_z$ is the transformed particle velocity in the z-direction. The delta function is the source term producing a discontinuity in $\breve{u}_z$ at a height of z_s. In order to solve the resulting equations, Lee et al. [4] used an analogy to a transmission line that results from the form of the transformed equation. The transformed equations have a very similar form to the "Telegrapher's Equation" of electrical transmission line theory. [4] Looking at the analogous telegrapher's equations,

$$\frac{dV}{dz} = -ZI(z) \tag{2.14}$$

$$\frac{dI(z)}{dz} = -Y(z)V(z) + I_o\delta(z - z_s) \tag{2.15}$$

there is a similar form of the equations if the shunt admittance $Y(z)$ is made a function of z and the series impedance Z a constant, with a current source at $z = z_s$. The equivalent transmission line configuration to Figure 2 is shown in Figure 3.
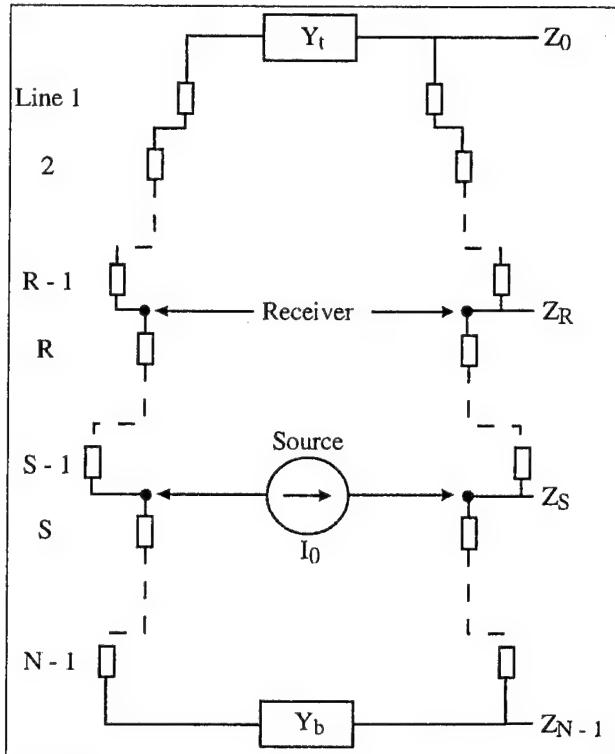
Figure 3. Transmission line analogy to the atmosphere.

Using the Lee et al. analogy, we can arrange the acoustic problem so that a solution can be calculated. We make the analogy by representing each layer in the atmosphere by an element in a transmission line with a certain characteristic admittance and attenuation constant. The admittance is defined as the inverse of the impedance or the inverse of the sum of the resistance plus the reactance of the electrical element. The admittance of the element causes the voltage running through it to be attenuated and causes a shift in phase of the signal. Viewing it from the perspective of the acoustic wave problem, the acoustic wave undergoes losses and phase shifting because of refraction and spreading of the acoustic wave as it propagates through the atmosphere. The equivalence between the transmission line and the acoustic wave problem is illustrated in Table 1. This equivalence can be performed for each layer of the atmosphere, thus constructing a transmission line. The top and bottom boundaries in the atmosphere become loading admittance elements on each end of the transmission line. Now the problem has been simplified to one of determining the voltage in the transmission line at a point in the line. This is a well-known process in electrical engineering.

Table 1. Transmission line analog relationships to acoustic fields

	Acoustic Wave	Transmission Line
Fields	Pressure $p(k,z)$	Voltage $V(z)$
	Velocity $\dot{w}$ (k,z)	Current $I(z)$
Attenuation Constant	$\Gamma = \sqrt{k^2 - (\omega / \alpha)^2}$	$\Gamma = \sqrt{ZI}$
Characteristic Admittance	$Y_c = -\Gamma / w\rho$	$Y_c = \sqrt{Y / Z}$

The zero-order Bessel function in Equation (2.10) can be expanded via Hankel functions:

$$J_o(\kappa r) = \frac{1}{2}\left[H_0^{(1)}(\kappa r) + H_0^{(2)}(\kappa r)\right]$$

(2.16)

The Hankel functions $H_o^{(1)}$ and $H_o^{(2)}$ represent incoming and outgoing acoustic waves, respectively. The FFP is designed to model radially outgoing acoustic waves. This allows for the first Hankel function to be suppressed with the additional argument that the incoming acoustic wave will not contribute significantly to the final result. The asymptotic expansion of the second Hankel function for large arguments is as follows:

$$H_o^{(2)}(\kappa r) \approx \sqrt{\frac{2}{\pi \kappa}} \frac{e^{-i(\kappa r - \pi/4)}}{\sqrt{r}} \quad \kappa r \gg 1$$

(2.17)

which makes the problem easier to handle. The important contributions from the integrand of the inverse transform, Equation (2.10), comes from the area where $\kappa < k_o$. Substituting Equation (2.17) into the inverse transform of Equation (2.10) and taking the far-field approximation, the acoustic pressure equation can be written as

$$p(r, z_r) \approx \frac{(1+i)}{\sqrt{2\kappa r}} \int_0^\infty \breve{p}(\kappa, z_r) e^{-\kappa r} \sqrt{\kappa} d \quad .$$

(2.18)

To perform the calculation on a computer, the continuous integral must be replaced by a numerical integral over discrete values of k. Applying this to Equation (2.18) yields

$$p(r, z_r) \approx \frac{(1+i)}{\sqrt{2} \ r} \Delta\kappa \sum_{n=0}^{N-1} \breve{p}(\kappa_n) \sqrt{\kappa_n} e^{-i(2\pi nm/N)}$$

(2.19)

in which

$$\Delta\kappa = \frac{\kappa_{max}}{N-1} \quad \kappa_n = n\Delta\kappa$$
$$m = \frac{r}{\Delta r} \quad \Delta r = \frac{2\pi}{N\Delta\kappa} .$$

(2.20)

The term κ_{max} comes from the property of the integrand of Equation (2.10) and only has significant contributions in a finite range of κ, allowing the summation to be terminated at a finite number of terms.

A problem in this representation of the solution is that $\breve{p}(k_n)$ is singular at some points along the real axis. These points represent modes propagating without attenuation. To avoid this difficulty, the current FFP uses "extra loss" in the calculations. The mathematical interpretation of using this extra loss is to move the numerical integration off the real axis. We remove the effect of the extra loss from the solution in an approximate manner by multiplying the computed pressure by the term $\exp(\alpha r)$, in which α is the extra loss attenuation constant in Np/m. It must be noted that the proper choice of this "artificial attenuation" is essential if meaningful results are to be obtained from the code.

7

Another problem with the numerical integration is the number of points, N, used in the summation of Equation (2.19). A lower bound on the number of points required in the summation is [6]

$$N_{min} = \frac{\kappa_{max} r_{max}}{\pi} \quad .$$

(2.21)

However, in most cases, this lower bound is too large to perform with a single FFT. The problem is how to have enough points to sufficiently sample the wave number space in the numerical integration. If Equation (2.19) is rewritten in the form

$$S = \sum_{n=0}^{N-1} G_n e^{-i(2\pi nm/N)}$$

(2.22)

this summation can be rewritten so that the single summation is rearranged to a double summation of the form:

$$S = \sum_{b=0}^{p} e^{-i[2\pi(b-1)m/p]} \sum_{n=0}^{N'-1} G_{n+(b-1)N} , e^{-[2\pi nm/(pN')]} \quad ,$$

(2.23)

in which $N' = N/p$ and p is an integer larger than 1. p is the number of panels into which the original FFT has been divided. Each panel contains N points. This technique allows the FFT to be performed to calculate the acoustic pressure with range at the height of the receiver.

2.3 Absorption of Sound by the Atmosphere

Viscosity, heat conduction, and molecular exchanges of energy basically cause losses in the medium. In the 19th century, the mechanisms of viscosity and heat conduction were the only ones suspected of causing dissipation of sound. Therefore, they are presently referred to as classical absorption.

In classical absorption, if one represents the effect of absorption by a factor $e^{-\alpha r}$ in which r is the distance of propagation, then the attenuation coefficient α_{cl} attributable to viscosity and heat conduction is given by Equation (2.17) from *Physical Acoustics XVII* [7]:

$$\alpha_{cl} = 5.57 \times 10^{-9} \frac{T/T_o}{T+110.4} \frac{f^2}{P/P_o} \quad .$$

(2.24)

The units of α_{cl} in Equation (2.24) are nepers/meter, in which P_o is the reference pressure of 1.01325×10^5 N/m^2 (1 atm), P is pressure in N/m^2, T_o is the reference temperature of 293.15K, T is the temperature in Kelvin, and f is the frequency in hertz.

In molecular absorption, energy exchanges at the molecular level include rotational and vibrational modes. Analysis of the rotational mode shows that its representative attenuation coefficient is proportional to α_{cl}, the classical attenuation coefficient:

$$\frac{\alpha_{rot}}{\alpha_{cl}} = 4.16 e^{-168 T^{-1/3}}$$

(2.25)

when 29K < T < 690K.

8

For frequencies below 10 MHz, it has been demonstrated that energy losses attributable to classical and molecular absorption are additive. A simplified empirical form of the equation can be written

$$\alpha_{cr} = 1.83 \times 10^{-11} \frac{\sqrt{T/T_o} f^2}{P/P_o} , \tag{2.26}$$

which is correct within 2% for 213K < T < 373K.

The vibrational mode of absorption should also be considered. Because the atmosphere is composed mostly of nitrogen and oxygen, each will contribute an attenuation coefficient. The vibration absorption is given by

$$\alpha_{vib,j} = \frac{4pX_j}{35c} \left(\frac{qj}{T}\right)^2 \frac{e^{-q_j/(Tf^2)}}{f_{r,j} + (f^2 / f_{r,j})} \tag{2.27}$$

in which j stands for either oxygen or nitrogen, X_j is the mole fraction of air component considered (0.20948 for oxygen and 0.78084 for nitrogen), q_j is the characteristic vibrational temperature (2239.1K for oxygen and 3352.0K for nitrogen), and c is the speed of sound at temperature T in m/s. The $f_{r,j}$ are the individual relaxation frequencies for oxygen and nitrogen. Computation of these depends on the relative humidity and atmospheric pressure. The relaxation frequencies are given by

$$f_{r,O} = \frac{P}{P_o}\left(24 + 4.04x10^4 h \frac{0.02 + h}{0.391 + h}\right) \tag{2.28}$$

$$f_{r,N} = \frac{P}{P_o}\sqrt{\frac{T_o}{T}}\left(9 + 280he^{-4.170(T_o/T)^{1/3} - 1}\right) \tag{2.29}$$

The total attenuation coefficient is then the sum of α_{cr} and $\alpha_{vib,j}$. Figure 4 is a log-log plot of total attenuation coefficient of T = 20 °C and Rh = 20%, adapted from reference [5]. It shows the contributions to attenuation from classical absorption, vibrational relaxation of nitrogen and oxygen, and the total attenuation coefficient attributable to the sum of these three attenuation mechanisms.
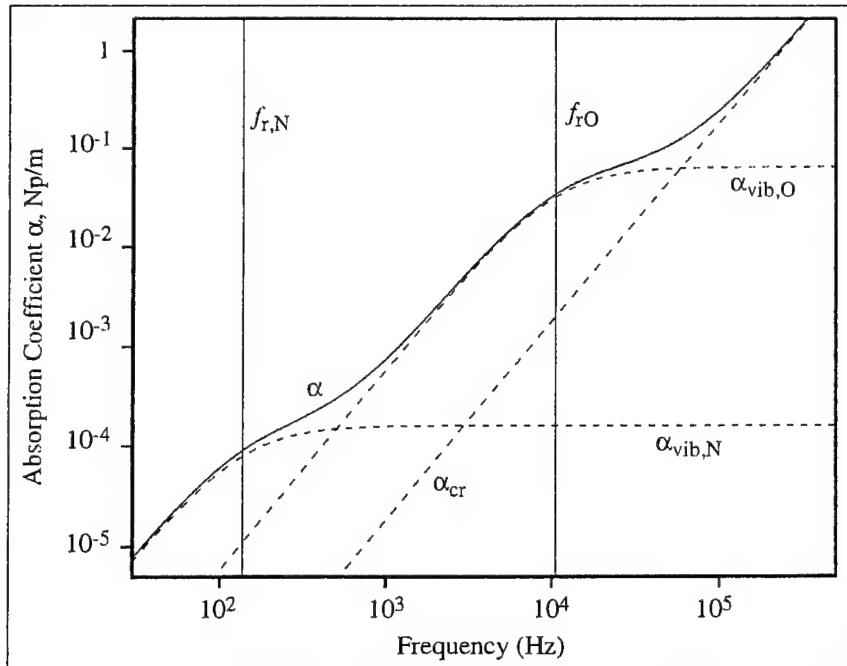
Figure 4. Log-log plot of sound absorption coefficient versus frequency for
sound in air at 20 °C at 1 atm pressure and with a water
vapor fraction h of 4.676×10^{-3} $(Rh = 20\%)$.

The attenuation coefficient α is roughly proportional to the square of the frequency. Thus, when frequency doubles, attenuation will quadruple. The attenuation of the sound wave attributable to molecular and vibrational absorption is very important for frequencies greater than or above 250 Hz. For frequencies below 250 Hz, this attenuation does not contribute much to the total attenuation of the sound wave.

2.4 Complex Ground Impedance

Several models are available for calculating the complex ground impedance. The impedance model used in WSCAFFIP is the Four-Parameter Model of Attenborough [8]. In this impedance model, the complex normalized characteristic impedance of the ground is calculated by

$$Z_c \cong \frac{\left[\dfrac{4q^2}{3\Omega} + i\dfrac{S_f^2 \sigma}{\omega \rho_o} \right]}{k_b} \tag{2.30}$$

in which $q^2 = W^{-n'}$, S_f is the pore shape factor ratio, Ω is the porosity of the ground, σ is the flow resistivity of the ground (mks) rayls, ω is the angular frequency $(2\pi f)$, ρ_o is the density of air (1.2 kg/m³), and k_b is the normalized wave number. The normalized wave number is computed from

$$k_b \cong \sqrt{\gamma \Omega} \left[\left(\frac{4}{3} - \frac{\gamma-1}{\gamma} N_{pr} \right) \frac{q^2}{\Omega} + i\frac{S_f^2 \sigma}{\omega \rho_o} \right]^{1/2} \tag{2.31}$$

in which γ is the ratio of specific heats, Equation (2.2), and N_{pr} is the Prandtl number (0.724).

10

The parameters S_f, Ω, ρ, and n' are normally varied until agreement is reached between impedance measurements and the impedance model is achieved. However, this method of determining the four parameters cannot always be completed if time or resources is lacking. To aid the user when the four parameters are unknown, there is a series of general descriptions of a variety of ground surfaces from which to choose. The user has the option to enter the values for the four parameters, if known.

Some ground surfaces have a layered structure that results from the gradual deposition of material over a soil base. Some examples are a layer of snow over frozen ground, decomposition of organic material over clay or sandy soil, or a well-plowed pasture over clay or harder packed soil. An effective impedance $Z(d)$ can be calculated for a semi-infinite layer of impedance Z_2 covered by a layer, depth d, or another material of impedance Z_1. The effective impedance is given by

$$Z(d) = \left[\frac{Z_2 - iZ_1 \tan(k_b d)}{Z_1 - iZ_2 \tan(k_b d)} \right] Z_1 \tag{2.32}$$

in which k_b is the bulk propagation constant in the top layer of the ground. The parameters Z_1, Z_2, and k_b are calculated by Equations (2.30) and (2.31) from Attenborough's Four-Parameter impedance model. In WSCAFFIP, the complex ground impedance is handled by the graphical user interface.

Table 2. Estimation of Ω and σ for various ground surfaces, given $n' = 0.750$ and $S_f = 0.875$

Description of Surface	Ω	σ(cgs)
Dry snow, new fallen 0.1 m over about 0.4 m old snow	0.850	23
Sugar snow	0.825	48
In forest, pine, or hemlock	0.825	48
Grass: rough pasture, airport, public buildings, etc	0.675	330
Roadside dirt, ill-defined, small rocks up to 0.1 m mesh	0.575	960
Sandy silt, hard-packed by vehicles	0.475	3470
"Clean" limestone chips, thick layer (0.01 to 0.025 m mesh)	0.425	6470
Old dirt roadway, fine stones (0.5 m mesh) intstices filled	0.400	7500
Earth, exposed and rain-packed	0.350	17100
Quarry dust, fine, very hard-packed	0.300	41700
Asphalt, sealed by dust and light use	0.250	120000

11

3. Built-in Features

3.1 Sound Speed Parser

As discussed in Section 2.2, the FFP uses constant sound speed layers. In previous versions of the propagation model, a novice running the model could induce error into the computation by having the atmospheric layer thickness too large. Also, previous versions of the propagation model used the entire meteorological profile regardless whether it was required to calculate the correct solution. Although this did not induce an error, the run time was slower since the run time depends on the number of layers in the profile. Thus, a *sound speed parser* was developed to mitigate these two problems. The parser runs invisibly to the normal user and yet provides a sound speed profile with the appropriate number of layers to the maximum height required to give a valid solution.

As Figure 5 shows, the deviation of a constant sound speed layer from the actual value of the sound speed is related to the slope of the sound speed profile. The larger the slope of the profile, the larger the difference of the true sound speed from the constant in the layer. We can minimize this by decreasing the thickness of the constant sound speed layer, but this can result in too many constant sound speed layers in the regions where the slope is very small. The layer thickness also depends on the wavelength. The shorter the wavelength, the smaller the layer thickness. By using the Green's Function Parabolic Equation (GFPE) model [9] as a comparison base, we ran
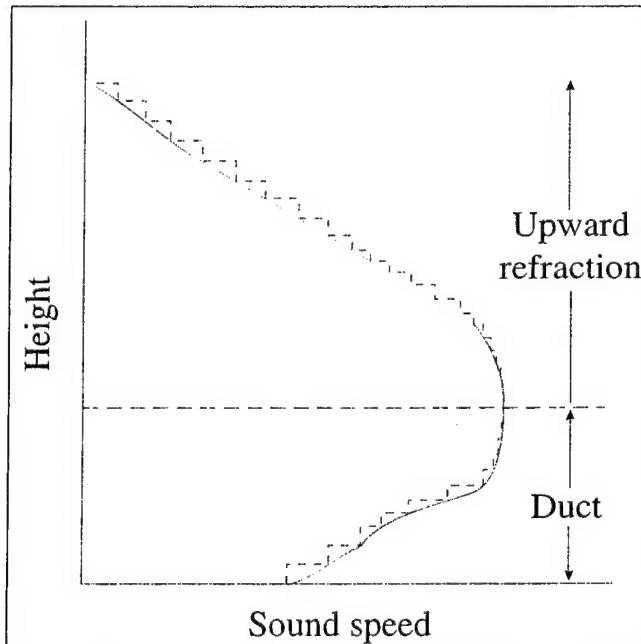

Figure 5. The difference between a real sound speed profile
(solid) and WSCAFFIP's interpretation (dashed)
of the sound speed profile.

WSCAFFIP using different layer thickness until a good comparison resulted between the two models. The resultant layer thickness was then used at different frequencies. After further adjustments, a ratio of the change in sound speed divided by the wavelength was found to give good results between the two models for different atmospheric profiles and frequencies. Figure 6 shows the result of having the layers too thick and shows the result of using the ratio technique. A ratio of 0.0125 was determined to give good results without slowing the calculation too much. The model uses this value when examining the sound speed profile and partitions the profile into thinner layers that do not exceed this value, if necessary.
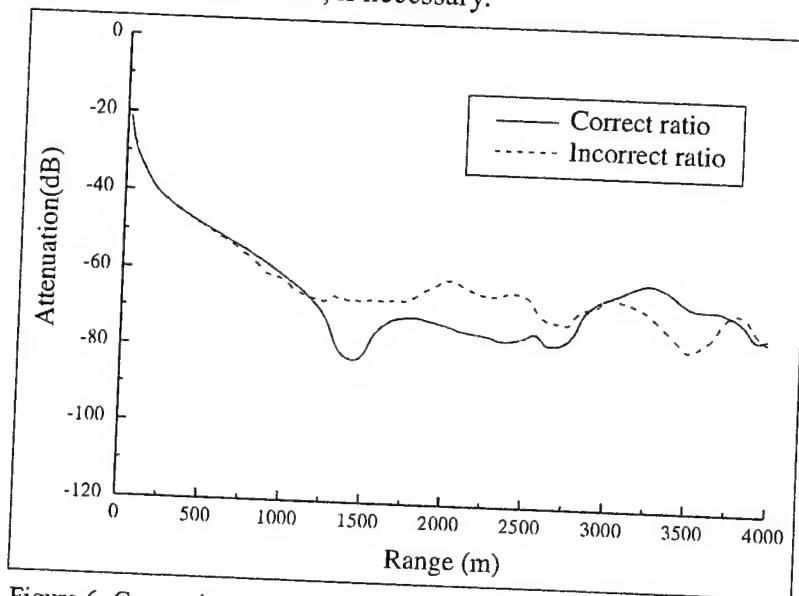

Figure 6. Comparison between two successive runs. (The solid line is using the correct ratio value and the dashed line is the incorrect value.)

Let us now consider the second function of the parser: truncating the sound speed profiles. Notice, with regard to Figure 5, that when the target and detector both lie within the duct, any sound propagating above the duct will not return since the region above the duct is all upward refracting. This means that using the entire profile is wasteful; any sound above the duct will stay above the duct and not affect the final solution. Since the shape of the sound speed profile changes with azimuth because of wind (see Figure 7), the maximum height required for the calculation varies with azimuth. Version 3.0 employs a simple approach to solving this problem. The simple assumption is to use the height where the highest value of the sound speed above the target and receiver occurs. This assumption is based on ray trace theory that suggests that no acoustic energy will contribute to the solution if the value of the sound speed at a given height and higher is always smaller than the sound speed at the receiver height of interest. This assumption normally works very well, but if the sound speed is close to the cut-off value of the sound speed, yet still smaller, acoustic energy returning from the heights higher than the cutoff does contribute to the solution. This is a manifestation of the difference between the ray and wave theory of acoustics. At this time, there is not a solution for this problem. However, it apparently does not appear very often. For insight into the calculation of profile height and number of layers, Appendix A contains brief descriptions of this subject in the discussion of the sample cases.
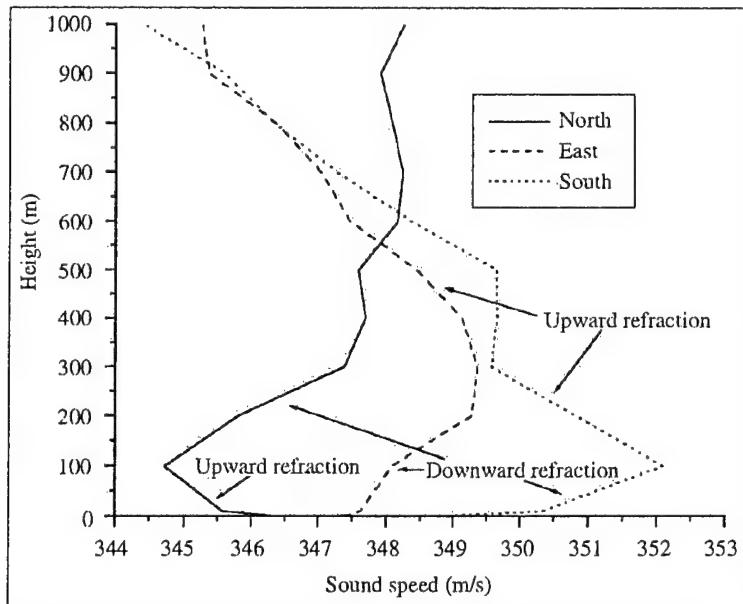
Figure 7. Sound speed profile to the north, east, and south of the target.

3.2 Output Smoothing

The attenuation of sound with range appears, as a simple curve with range, or a very complex structure, depending on the number of paths in the atmosphere for the sound to reach the receiver and on the various modes of propagation present (surface wave, creeping wave, diffraction, etc.). Figure 8 shows an example of the complex structure of the attenuation of sound with range. When experiments are typically performed in the atmosphere, it is very difficult to measure the exact, complex structure. This is because the atmosphere is dynamic. Atmospheric turbulence is constantly varying the temperature, wind speed, and wind direction. This results in continually changing fine structure in the attenuation curve. However, since acoustic sensor systems record a time average of the signal, much of the changing fine structure will average. This is the reason for adding the output smoothing. The model performs an 11-point average on the attenuation of sound with range. This acts as a low-pass filter to average the high frequency variations in the output. The high frequencies refer to the oscillations in the attenuation curve not in the acoustic signal. This technique provides for a much cleaner graph of the results of the calculation. Figure 9 shows the same case as Figure 8 except with smoothing turned on. There is an option available to switch the smoothing off if one is interested in noting the difference it makes in the quality of the output graph. Future versions of our models that will include turbulence will be able to provide additional information about the bounds of the amplitude fluctuations and the bearing errors.

14
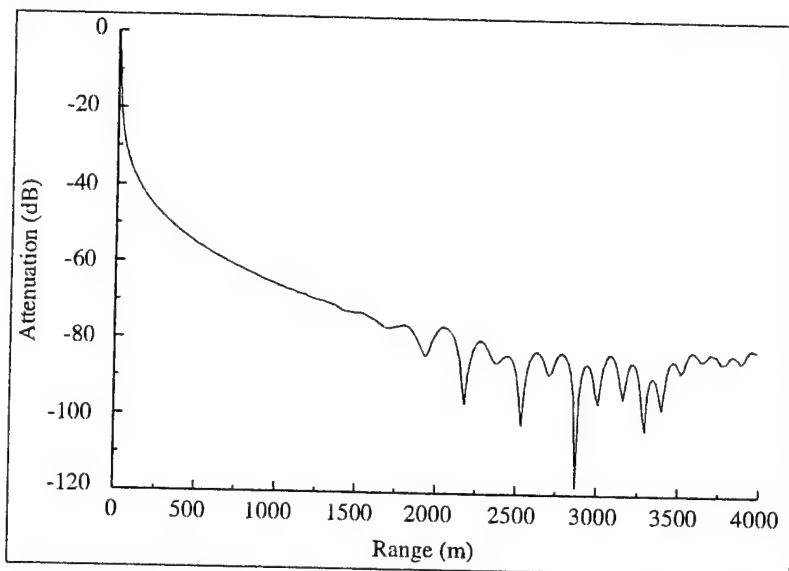
Figure 8. Attenuation versus range with smoothing turned off.
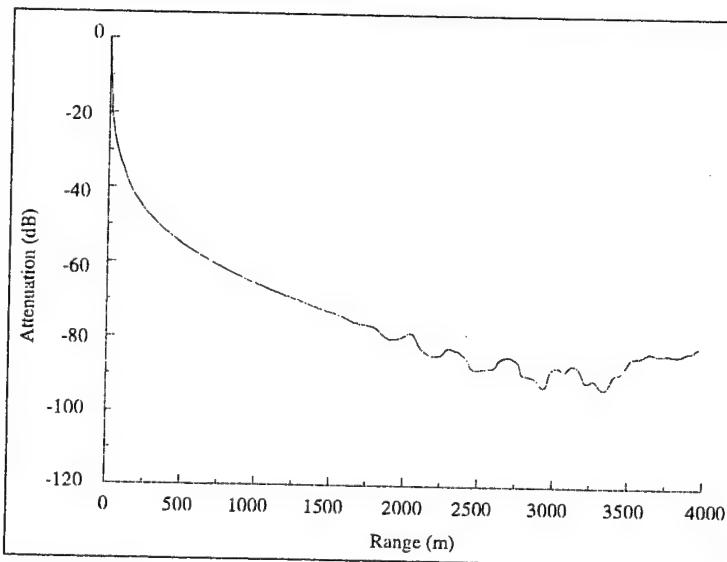
Figure 9. Attenuation versus range with smoothing turned on.

3.3 Meteorological Profile Builder

Since the atmosphere plays a significant role in affecting the propagation of sound, knowing the state of the atmosphere is critical in performing a model calculation. Since users may not have meteorological profiles available to them for every location, a meteorological profile builder was developed to give the user a tool to create his/her own profiles, based on basic information. The profile builder is not sufficient to generate profiles for calculations at large distances (> 5 km). This is because of the assumptions upon which the profile builder is based. For long-range propagation calculations, a more dynamic meteorological profile model must be used.

15

In the surface layer, mechanical and thermal forcing are the primary driving forces. Monin Obukhov introduced scaling parameters that allow the state of the atmosphere to be described, which were independent of height. The scaling parameters are the friction velocity (u_*), scaling temperature (T_*), and the scaling length (L) with a normalized height $\zeta = z/L$. The temperature and wind speed profiles are calculated by [10]

$$u(z) = \frac{u_*}{k}\left[\ln\left(\frac{z}{z_o}\right) - \Psi_M(z/L) + \Psi_M(z_o/L)\right] \tag{3.1}$$

$$T(z) = T(z_t) + \frac{T_* P_t}{k}\left[\ln\left(\frac{z}{z_t}\right) - \Psi_H(z/L) + \Psi_H(z_t/L)\right] \tag{3.2}$$

in which k is the von Karman's constant (0.4), z_o is the aerodynamic roughness length, z_t is an arbitrary height, and $P_t = 0.74$. The universal functions used in this development are

$$\Psi_M(\zeta) = \Psi_H(\zeta) = \frac{3}{2}\ln\left(\frac{1-\phi^{-1}+\phi^{-2}}{3}\right) + \sqrt{3}\tan^{-1}\left(\frac{2\phi+1}{\sqrt{3}}\right), \qquad \zeta < 0 \tag{3.3}$$

$$\Psi_M(\zeta) = \Psi_H(\zeta)/P_T = -4.7\zeta, \qquad \zeta < 0 \tag{3.4}$$

in which

$$\phi_M(\zeta) = \begin{cases} (1-15\zeta)^{-1/3} & \zeta < 0 \\ 1+4.7\zeta & \zeta > 0 \end{cases}$$
$$\phi_H(\zeta) = \begin{cases} (1-9\zeta)^{-1/3} & \zeta < 0 \\ 1+(4.7/P_t)\zeta & \zeta > 0 \end{cases} \tag{3.5}$$

The problem is, what are good values for the friction velocity, scaling temperature, and scaling length for different locations, time of day, and seasons of the year? In order to determine these parameters, the energy balance model developed by Rachele and Tunick [11] was employed. The model balances the energy flux at the soil surfaces as

$$R_N = H + L'E + G \tag{3.6}$$

In which R_N is the net radiative flux, H is the turbulent sensible heat flux, $L'E$ is the latent heat flux attributable to surface evaporation, and G is the flux of heat into the soil. Each term in the equation reduces to the basic measurable quantities. R_N can be expressed as the sum of the fluxes of the net shortwave and net longwave radiation. The energy balance model is constrained to require a minimum number of conventional meteorological inputs from a 2-m reference level. The input includes temperature, pressure, relative humidity, and wind speed. The model also requires a judgment of the soil type and moisture, cloud characteristics, day of the year, time of day, and longitude and latitude of the site of interest. Nearly all this input is measured for most areas of the world, and charts are available to estimate the soil characteristics. Appendix C provides the user with a series of tables to choose some of the parameters that cannot be directly measured such as

16

albedo, soil characteristics, etc. Using this input, the energy balance model calculates the similarity parameters required to calculate the temperature and wind speed profile required by the acoustic propagation model.

3.4 Run Options

WSCAFFIP offers the user the ability to set program flags that modify how certain calculations are made and generate additional output files. In the current version, there are several run options: source to receiver, receiver to source, output sound speed profile, disable smoothing, generate Battlefield Acoustic Simulation System (BASS) output file, output ray information, and change the units of some of the meteorological input. The default configuration is for source to receiver, output sound speed profile, atmospheric pressure in millibars, wind direction in degrees, and temperature in Celsius. Here is a description of each run option:

source to receiver: The sound is attenuated from the source to the receiver. This is used when the user wants to view the sound attenuation from a source (i.e., tank, helicopter, etc.)

receiver to source: The sound is attenuated from the receiver to the source. This is used when the user wants to view the sound attenuation from a sensor (i.e., WAM, AHM, etc.)

output sound speed profile: Allows the user to output the sound speed profile along the selected bearing for the given meteorological profile. This option generates three output files: sound.o, sound.new, and sound.inf. The first file, sound.o, is the sound speed profile calculated from the meteorological profile input to WSCAFFIP. The second file, sound.new, is the sound speed profile used by WSCAFFIP to perform its calculations. This profile was generated by the sound speed parser (see Section 3.1). The last file, sound.inf, was also generated by the sound speed parser. The file gives some basic analysis of the sound speed profile examined. The file formats for the three files are given below:

File Name: sound.o (Original Profile)

Format:

$Z(1)$	$C(1)$
$Z(2)$	$C(2)$
M	M
$Z(Nint)$	$C(Nint)$

in which Nint is the number of interfaces, $Z(i)$ is the height of the ith interface in meters and $C(i)$ is the sound speed of the ith interface in m/s.

File Name: sound.new (Parsed Profile)

Format:

```
Z(1)   C(1)
Z(2)   C(2)
 M      M
Z(N)   C(N)
```

in which N is the number of interfaces in the new profile.

File Name: sound.inf (Parsed Profile Analysis)

Format:

Results of Profile Parsing

Sound Speed at the surface: 342.42 m/s

Sound Speed at top of profile: 329.83 m/s

Height of profile: 1327.00 m

Largest sound speed 342.42 m/s occurred at 0.00 m

Sound speed at source: 340.58 m/s   Sound speed at sensor: 342.42 m/s

Highest ray: 30.00 m

Top of new profile: 382.00 m

Detector just outside the atmospheric duct.

Maximum height was reset to capture leakage from the duct.

Duct Height: 382.00 m with sound speed of 338.22 m/s

Possible Sound Ducts Found

Number of ducts: 3

Duct \#1 - c: 341.955361 z: 172.000000 dz: 172.000000 index: 7

Duct \#2 - c: 338.222784 z: 382.000000 dz: 182.000000 index: 13

Duct \#3 - c: 338.158191 z: 450.000000 dz: 50.000000 index: 15

Number of layers in original profile: 27

Number of layers in new profile: 741

disable smoothing: As discussed in Section 3.2, WSCAFFIP smoothes the higher frequency variations in the attenuation table. This option allows the user to switch the smoothing off if the case requires it.

generate BASS output file: If the user needs to provide attenuation tables for the older BASS sensor performance model, selecting this option will generate an additional file named proptab.dat. This file has the format of

<u>Format</u>:

$$
\begin{array}{cccc}
dB(1,1) & dB(2,1) & L & dB(M,1) \\
dB(2,1) & dB(2,2) & L & dB(M,2) \\
M & M & O & M \\
dB(1,N) & dB(2,N) & L & dB(M,N)
\end{array}
$$

in which N is the number of range points, M is the number of frequencies, and $dB(j,i)$ is the relative sound level at the ith range and jth frequency in decibels (re: 20 µPa).

output ray information: As part of the sound speed parser, a ray trace calculation is made to determine some characteristics of the atmosphere. The rays generated by the routine can be sent to a file named "rays.out" if the user would like to use this information.

pressure in millibars: The current version has changed the default units used for the atmospheric pressure. WSCAFFIP now defaults to use millibars as the measure of atmospheric pressure. To be compatible with older meteorological profiles, this flag was provided. If the user is using an older meteorological profile, which employs atmospheres as the measure of atmospheric pressure, just unset this flag to correctly read the file. This change was made to better match the pressure units normally measured by meteorological teams in the battlefield.

WSCAFFIP uses an array of flags to internally handle the run options. This array of flags can be seen in the configuration file. The first line in the configuration file is a "printout" of the flag array. In the current version, there is allocation for as many as 16 run flags; however, only eight flags are currently used. The remaining eight flags are for future use. A 0 indicates the flag is off, and a 1 indicates the flag is on. The order of the flags is

Flag Number	Function
0	output sound speed profile
1	wind direction in degrees
2	source-to-receiver/receiver-to-source
3	reserved
4	reserved

5	reserved
6	reserved
7	reserved
8	disable smoothing
9	generate BASS output file
10	pressure in millibars
11	temperature in Celcius
12	output ray information
13	output ray information
14	reserved
15	reserved

4.   Operations

4.1   Installing WSCAFFIP

There is little to do for the installation. WSCAFFIP typically is sent as a self-extracting archive.
The user runs the progam. The extractor will ask for the directory in which to place to extracted
files. If the installation is a regular pkzip file, use pkunzip to extract the files into the directory
where the program will operate. The archive contains four files: wscaffip.exe, proptab.pth,
proptab.ptd, and wscaffip.hlp, with a sample directory containing the files for Appendix A. These
files will be extracted to the directory the user has created to store the program. The proptab.pth
and proptab.ptd files contain the header information and attenuation table. The wscaffip.hlp file
contains some basic help information. These three files must be situated within the WSCAFFIP
directory for the program to work correctly.

4.2   How to Run WSCAFFIP

When the user runs WSCAFFIP, the program will display the window shown in Figure 10. All the
user-required information is given under the "Model Inputs" menu. There are five selections to be
made: meteorological profile, geometry, target frequency, ground characteristics, and run options.
When the user runs the program, a default case initializes the propagation model. The user can
reset the program back to the run-time defaults by selecting the default settings. Appendix A
shows the default settings.

20
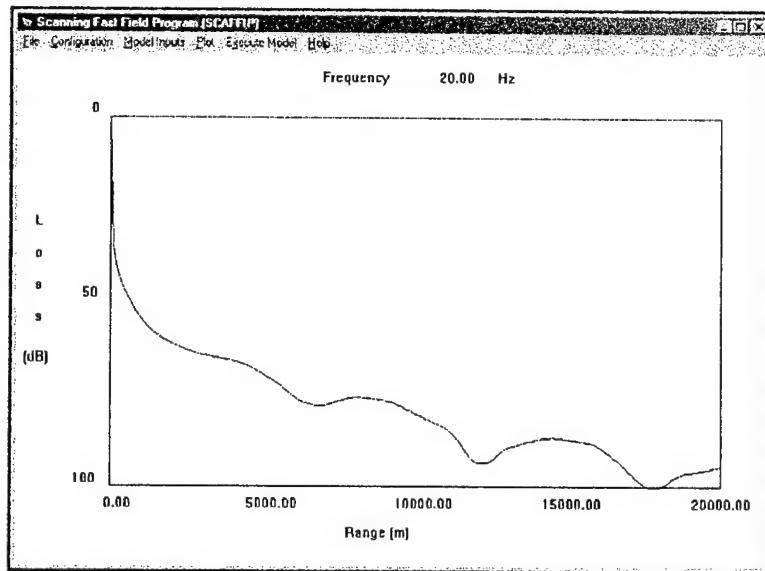
Figure 10. WSCAFFIP run time window.

The meteorological profile input gives the user three options from which to choose: open profile, use a standard meteorological case, and create a meteorological profile. The open profile is used when a meteorological profile is available. The format of the meteorological file is listed below:

Format:

Nint

Z(1)	T(1)	Rh(1)	P(1)	Wvel(1)	Wdir(1)
Z(2)	T(2)	Rh(2)	P(2)	Wvel(2)	Wdir(2)
M	M	M	M	M	M
Z(Nint)	T(Nint)	Rh(Nint)	P(Nint)	Wvel(Nint)	Wdir(Nint)

in which Nint is the number of interfaces, $Z(i)$ is the height of the ith interface in meters also $Z(1) = 0$ and $Z(i) < Z(i+1)$ always, $T(i)$ is the temperature in Kelvin, $Rh(i)$ is the relative humidity in percent, $P(i)$ is the atmospheric pressure in millibars, $Wvel(i)$ is the wind speed in meters per second, and $Wdir(i)$ is the wind direction in degrees, from which the wind is blowing relative to north. Each meteorological value is measured at height $Z(i)$. Choosing the open profile selection displays the open meteorological profile window, as shown in Figure 11. The selected profile will be read and used to perform model calculations.

21
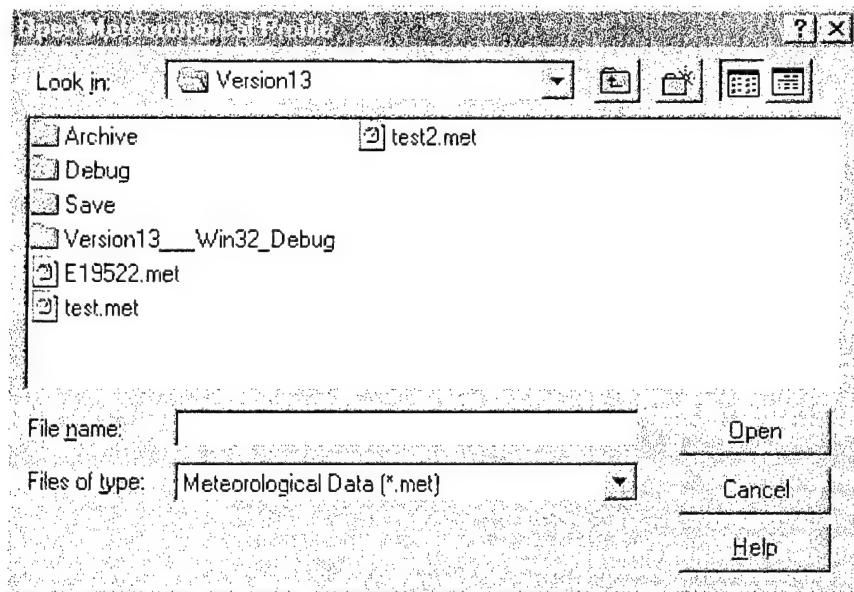
Figure 11. Open meteorological profile window.

The next way of obtaining a meteorological profile is to select the standard meteorological cases: overcast/calm, overcast/windy, sunny/calm, sunny/windy, night/calm, and night/windy (see Figure 12). The six cases represent typical cases that the user would observe. Once the user selects a standard case, s/he has to enter the temperature, relative humidity, and wind direction to complete the required input. If the user would like to further customize the values after pressing OK, s/he
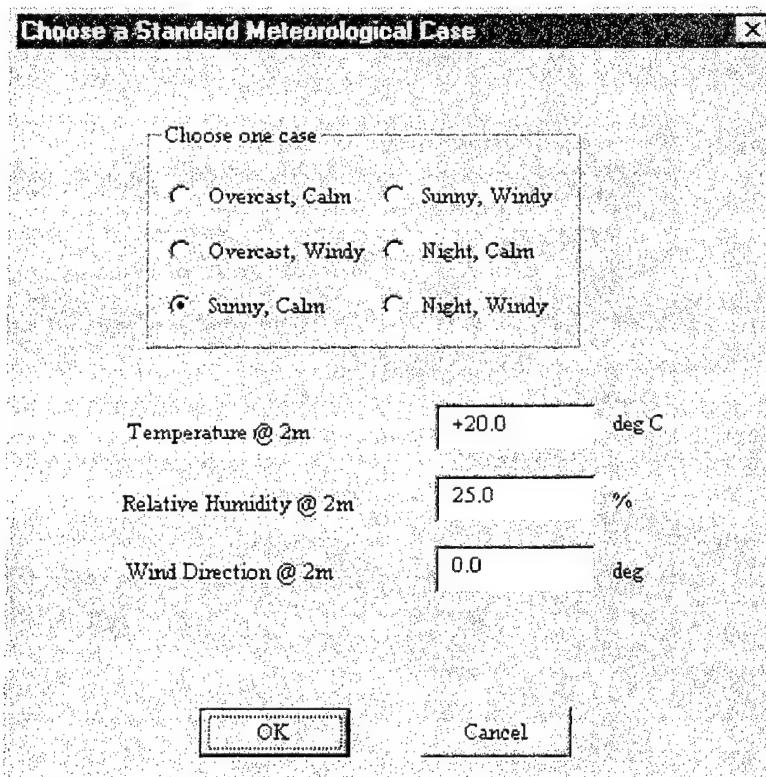
Figure 12. Standard meteorological profile window.

can select "create a meteorological profile." The setting for the standard profile case will be copied to the "create profile" windows. To use the "create profile" windows, refer to Section 4.3. Selecting the OK button results in the creation of a meteorological profile.

Next, choose the target frequency input selection. There are three choices to specify the frequency parameters (see Figure 13): starting frequency, ending frequency, and frequency resolution. The starting frequency is the first frequency used in the frequency sweep. The ending frequency is the cut-off frequency for the sweep. The frequency resolution is the interval between frequencies in the sweep. The current version of WSCAFFIP does not allow for the frequency resolution to be 0. If the user wants to run one frequency, s/he must input the same value for the starting and ending frequencies and give a non-zero positive number for the resolution.
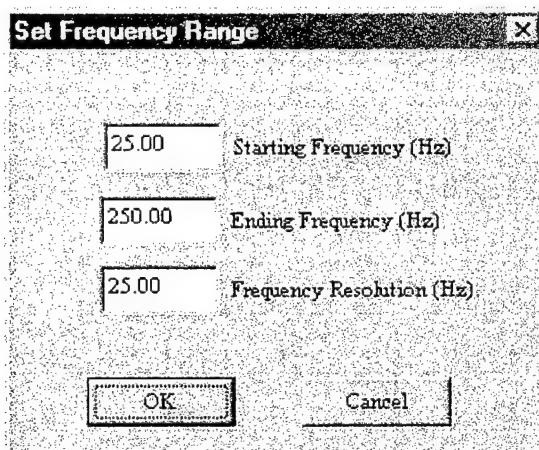
Figure 13. Frequency input menu.

The next input selection is the ground characteristics. The options for this are shown in Figure 14. WSCAFFIP gives the user several different types of grounds and ground conditions from which to choose. The selection here will generate a value for the ground impedance used by the propagation model; see Section 2.4 for further information. A future version will allow the user to specify parameters for the ground impedance model.

23
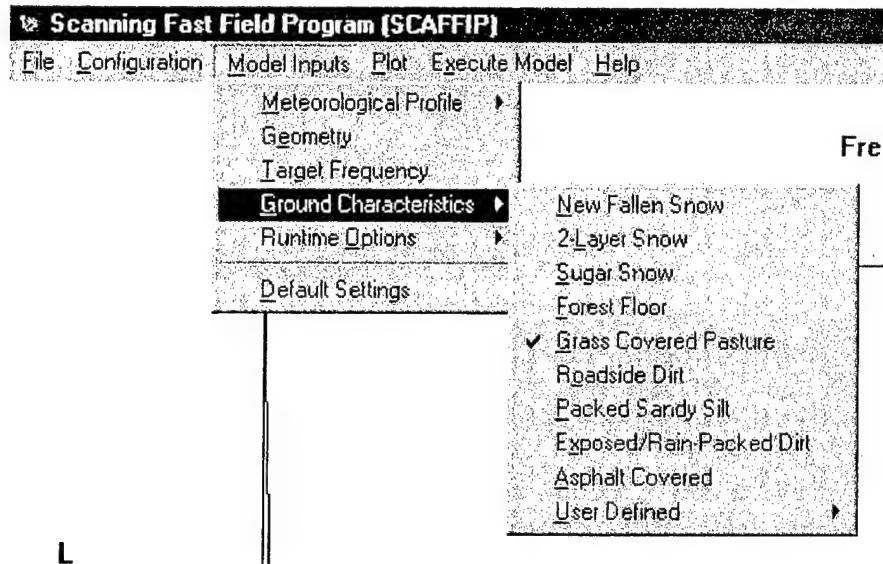
Figure 14. Ground impedance input menu.

The last input selection is the run options. The options for this are shown in Figure 15. These input parameters allow the user to modify how the model runs and generate additional output information. The details of the options and the default values are discussed in Section 3.4.
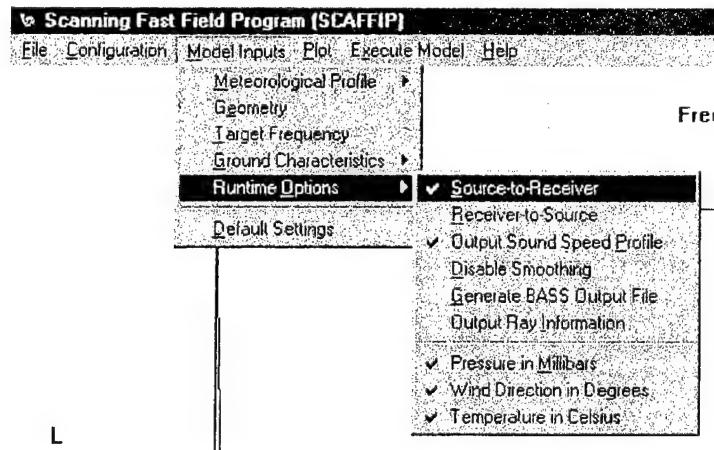

Figure 15. Frequency input menu.

Once all the input is given under the five sections, the user is now ready to run the propagation model to generate an attenuation table. To do this, s/he must select the execute model menu item. This will display a window (see Figure 16), notifying the user that it may take some time to perform a calculation and asking the user whether to continue. If the user presses the "yes" button, the propagation model will execute. The length of time to perform a calculation varies, depending on the height of the meteorological profile, number of interfaces in the profile, number of frequencies, frequency values, and propagation range. Run tables are provided with each sample case in Appendix A. The current version of WSCAFFIP may slow or lock the windows until the calculations are complete. Future versions will provide an indication that the program is still executing.

24
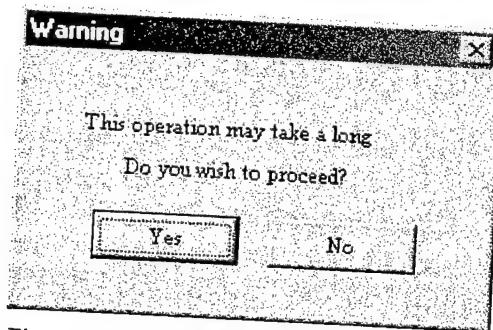
Figure 16. Model execution warning.

4.3 How to Run a Meteorological Profile Builder

The meteorological profile builder is divided into two parts: basic and advanced. The basic window (see Figure 17) appears to the user when s/he selects the "create a meteorological profile" option from the model input/meteorological profile menu. This window contains the minimal information that the user must give the profile builder. The longitude, latitude, time of day, and day of the year are used to calculate the solar angle. The solar angle and cloud cover determine the amount of solar radiation reaching the ground. The remaining four parameters determine the meteorological parameters used to generate the meteorological profile. The basic profile calculation assumes that the location is at sea level, the ground is covered with low grass, and the soil is moist.

Figure 17. Meteorological profile builder window.

To alter these assumptions, the user must select the advanced button on the "build a meteorological profile" window. This creates another window shown in Figure 18. This window contains additional parameters that the user can use to customize the meteorological profile. Most of the parameters on this window require the user to have advanced knowledge about the environment. To aid the user in selecting values for this window, a series of tables has been provided in Appendix B. The tables will allow the user to select the values required to customize the profile builder to his/her scenario. Once all the parameters have been entered, the user generates the profile by selecting the OK button in each of the profile builder windows.
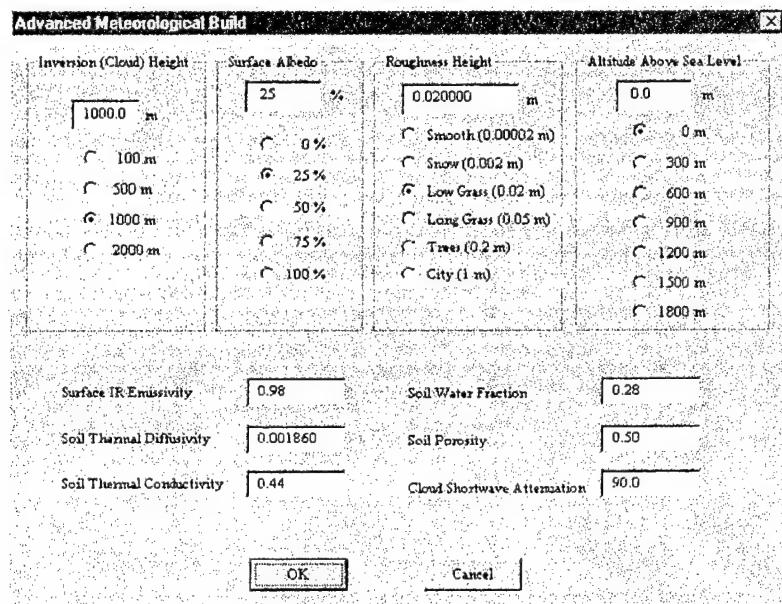
Figure 18. Advanced meteorological profile builder window

The generated profile is not automatically saved to a file. It resides in memory by default. It is recommended that the user employ the save option under the model input/meteorological profile/ create a meteorological profile to store the profile to a file for later use. This way, the user will not lose the profile in case the program abnormally terminates. If the user wishes to use the profile in the future, s/he just has to read the profile back into memory.

4.4   Additional Features

In addition to the features described so far, WSCAFFIP also offers the user some additional capabilities: store/retrieve/view configurations, save/retrieve attenuation table, and print attenuation plots to a laser printer. The program has been tested on most types of HP-compatible laser and ink jet printers.

In order to preserve the user's settings, WSCAFFIP allows the user to save the current input configuration into a file. Under the configuration menu, there are three options: open, save, and view. Open allows the user to open and read a previously stored configuration file. Save will store the current configuration into a file. The view option allows the user to see the values selected for the propagation model (see Figure 19). The configuration file is ASCII with the format:
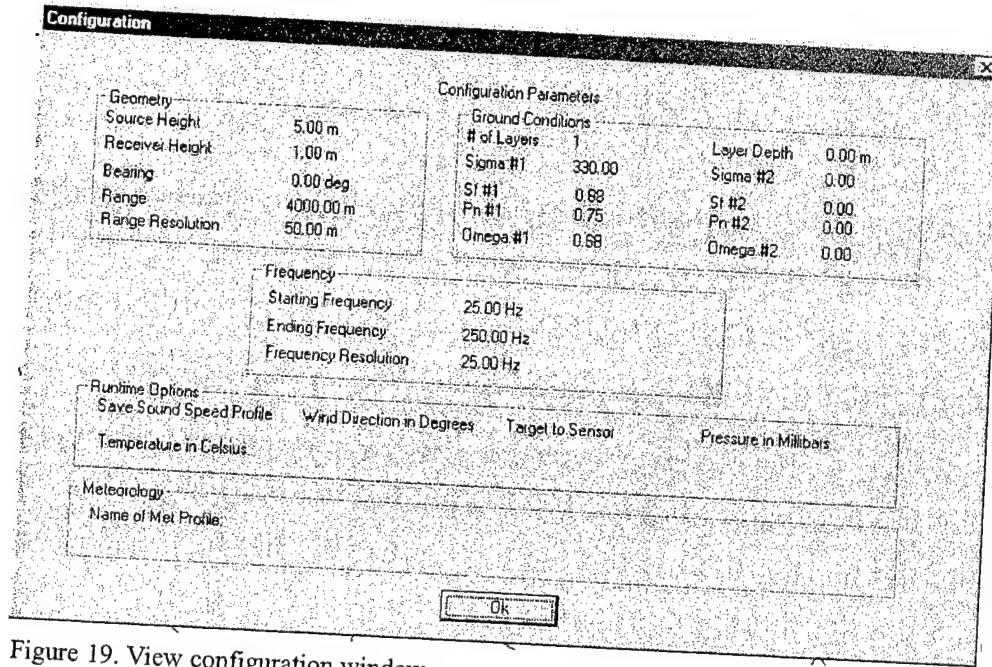
Figure 19. View configuration window.

Format:

// Configuration File for WSCAFFIP v3.0

// Run Options

options

// Geometry

// Source Height (m) Receiver Height (m) Bearing (deg)

Zsrc Zdet q

// Range (m) Range Resolution(m)

R D R

// Frequency

// Start Freq (Hz) Stop Freq (Hz) Freq Resolution (Hz)

f1 f2 D f

// Ground

// Number of Layers Layer Depth (???)

Ngnd dgnd

// Sigma1 Sf1 Pn1 Omega1

*s*1 *sf*1 *Pn*1 W1

// Sigma2 Sf2 Pn2 Omega2

*s*2 *sf*2 *Pn*2 W2

// Ground Flag

gndflag

// Meteorology

// Meteorological Profile Options

metflag1

metflag2

// Size of File Buffer

buffer

// Name of Meteorological Profile

metname

// Plot Title

title

in which run options are the 16 binary flags defining what options have been set. See Section 3.4 for a list of the options. Z_{src} is the height of the target in meters, Z_{det} is the height of the detector in meters, q is the bearing in degrees, R is the maximum range of interest in meters, DR is the range step in meters, f_1 is the starting frequency in hertz, f_2 is the ending frequency in hertz, Df is the frequency steps in hertz, N_{gnd} is the number of ground layers (0 or 1), d_{gnd} is the depth of the top layer in meters, s_1 is the flow resistivity in cgs units of the top layer, sf_1 is the pore shape factor of the top layer, Pn_1 is the grain shape factor of the top layer, W_1 is the porosity of the top layer, s_2 is the flow resistivity in cgs units of the bottom layer, sf_2 is the pore shape factor of the bottom layer, Pn_2 is the grain shape factor of the bottom layer, W_2 is the porosity of the bottom layer, gndflag is the type of ground surface used in calculation, metflag1 is the meteorological profile option selected, metflag2 is the flag indicating that the meteorological profile was read from a file, and metname is the name of the meteorological profile used for the calculation. If the profile was generated by the profile builder, this field will be blank.

4.5   Format of Output Files

Two output files are produced by the program. The first is the attenuation table called proptab.ptd that is an ASCII table with a format of

Format:

0	freq(1)	freq(2)	L	freq(M)
R(1)	dB(1,1)	dB(2,1)	L	dB(M,1)
R(2)	dB(2,1)	dB(2,2)	L	dB(M,2)
M	M	M	O	M
R(N)	dB(1, N)	dB(2, N)	L	dB(M, N)

in which N is the number of range points, M is the number of frequencies, and dB(j,i) is the relative sound level at the ith range and jth frequency in decibels (re: 20 μPa). The other output file is a header file called proptab.pth providing information about the attenuation table. The format of the header file is

Format:

// Propagation Table Header

//

// Created by WSCAFFIP

//

// ID String

Generated by WSCAFFIP

// Prop Data Table name

proptab

// Prop direction re wind

propdir

// Number of ranges (rows) in prop table

nranges

// Number of frequencies (columns) in prop table

nfreqs

// Atmospheric Conditions File

// c(z) data table

// Number of heights (rows in c(z) table

0

// Zmax (0 if unknown)

0

in which proptab is the name of the file containing the propagation table with the extension .ptd, propdir is the propagation direction relative to the wind in degrees, nranges is the number of ranges, and nfreqs is the number of frequencies. The remaining four fields are not implemented in the current version of WSCAFFIP. The default names for the attenuation table and header are proptab.ptd and proptab.pth, respectively. These names can be changed with the file/save table option. The extensions need to remain the same in order to be compatible with input into other sensor performance programs.

---

5. Future Revisions

This is the last planned major revision of WSCAFFIP. Planned future revisions will be to eliminate any "bugs" found and to optimize the program to work with Microsoft Windows. The future model development will focus on the parabolic equation (PE)-based propagation models such as the Finite Element PE (FEPE), Crank-Nicolson PE (CNPE), and the Green's Function PE (GFPE). The PEs are more robust, allowing for incorporation of additional environmental effects on sound propagation. The PEs were not initially used because of several difficulties in the operation of these types of models. The FEPE and CNPE are very computationally intensive, limiting the frequency that the user could practically run. The GFPE solves these problems, but some of the additional input parameters were difficult for the non expert user set. The incorrect parameters would result in incorrect results, which a non-expert in propagation models could interpret as errors. However, the newer version of the GFPEs is greatly improved, and many of the input parameters can be parameterized and automated, based on the typical information that the user has available. The GFPE will allow for incorporation of scattering from atmospheric turbulence and irregular terrain. The first version will be named "SCAPE" (Scanning Parabolic Equation). The user interface and capabilities will be similar to WSCAFFIP. The main difference between the two is that SCAPE will allow the user to calculate an attenuation table for several heights simultaneously instead of only one height like WSCAFFIP. The first version of SCAPE software is available.

References

1. F. R., Naval Underwater Systems Center, "A Fast-Field Program for Multilayered Media," Technical Report 4103, 1971.

2. H. W. Kutschale, "The Integral Solution of the Sound Field in Multilayered Liquid-solid Half-space with Numerical Computations for Low-frequency Propagation in the Arctic Ocean," Report No. 1 (CU1-1-70, ONR Contract N00014-67-A-0108-0016), Lamont-Doherty Geological Observatory, Columbia University, Palisades, NY, 1970.

3. R. Raspet, W. Lee, E. Kuester, D. C. Chang, W. F. Richards, R. Gilbert, and N. Bong, "Fast-field Program for a Layered Medium Bounded by Complex Impedance Surfaces," *J. Acoust. Soc. Am.* **77**: 345–352, 1985.

4. W. Lee, N. Bong, W. F. Richards, and R. Raspet, "Impedance Formulation of the Fast-field Program for Acoustic Wave Propagation in the Atmosphere," *J. Acoust. Soc. Am.* **79**: 628–634, 1986.

5. Allen D. Pierce, *Acoustics: An Introduction to Its Physical Principles and Applications*, McGraw-Hill, New York, 1981.

6. S. J. Franke and G. W. Swenson, Jr., "A Brief Tutorial on the Fast-field Program (FFP) as Applied to Sound Propagation in the Air," *Applied Acoustics* **27**: 203-215, 1989.

7. *Physical Acoustics XVIII*, edited by Mason and Thurston, Academic Press, New York, 1984, pp. 145–232.

8. K. Attenborough, "Acoustical Impedance Models for Outdoor Surfaces," *J. Sound Vib.* **99**: 521–544, 1985.

9. Kenneth E. Gilbert and Xiao Di, "A Fast Green's function method for one-way sound propagation in the atmosphere," *J. Acoust. Soc. Am* **94**: 2343–2352, 1993.

10. A. L' Espérance, J. Nicolas, D.K. Wilson, D.W. Thomson, Y. Gabillet, and G. Daigle, "Sound Propagation in the Atmospheric Surface Layer: Comparison of Experiment with FFP Predictions," *Applied Acoustics* **40**: 325–346, 1993.

11. Henry Rachele and Arnold Tunick, "Energy Balance Model for Imagery and Electromagnetic Propagation," *Applied Meteorology* **33**: 964–976, 1994.

Appendix A. Sample Case

This appendix provides a sample case against which the user can compare his or her version of the code. This aids in determining whether the code was installed correctly and training for the new user. The meteorological data and configuration files for the case were provided with the program code. The sample case will also be used to illustrate some of the environmental effects on sound propagation. Since the meteorological data file will be provided with the program, tabulation of the input data will not appear in this appendix as in previous user manuals.

For this case, the meteorological profiles of temperature, wind speed, and wind direction are shown in Figures A-1 through A-3, respectively. This surface wind is light from the northeast. There is a low-level wind jet (local maximum in the wind speed) at 100 m and the wind direction is from the northwest. The effect of this low-level wind jet will be obvious when the sound speed profile is examined. As can be seen in the wind speed profile, there is a shift in the wind direction at the top of the temperature inversion from the north to the southeast. Figure A-4 shows the sound speed profile in three directions: north, east, and south. This represents propagation up-wind, crosswind, and downwind.
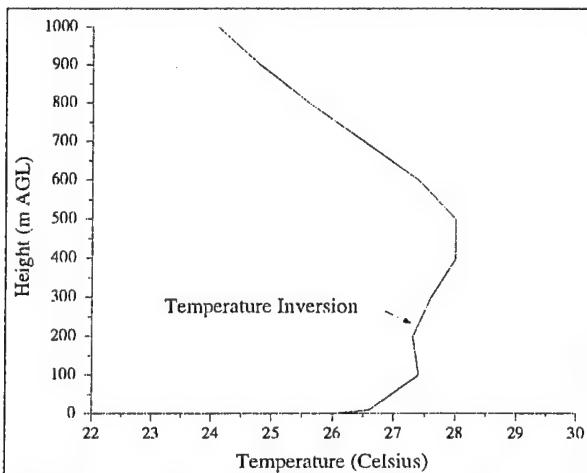

Figure A-1. Temperature profile.
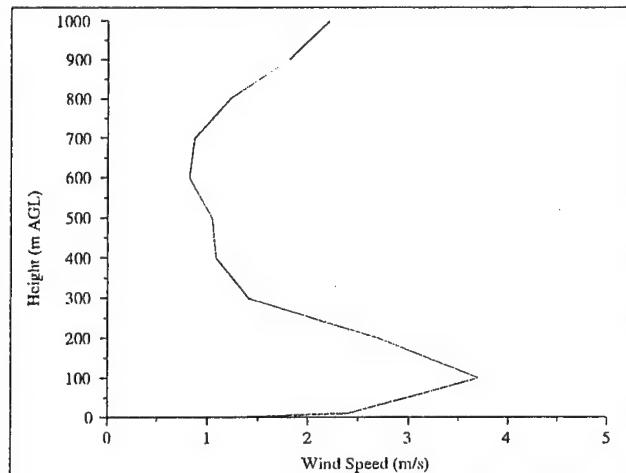

Figure A-2. Wind speed profile.
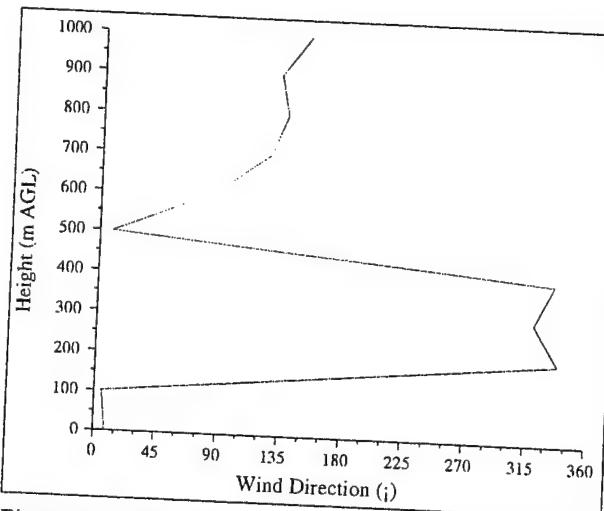
Figure A-3. Wind direction profile.
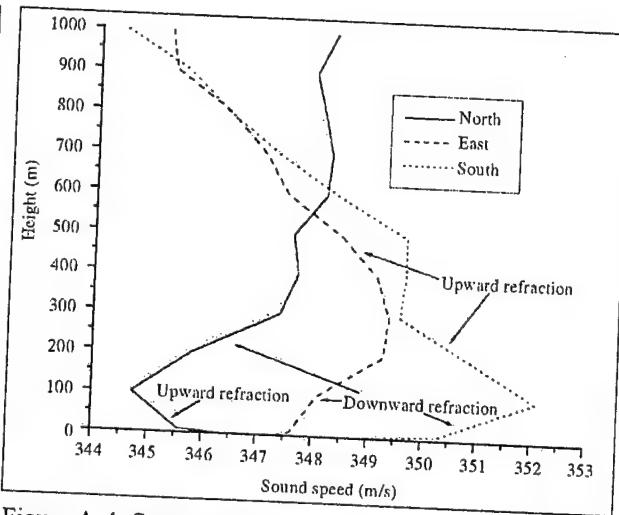
Figure A-4. Sound speed profile to the north,
east, and south of the target.

The sound speed profile provides a wealth of information. Looking at the sound speed profile to the north (0 degrees), the sound speed is decreasing with height indicating upward refraction, thus poor propagation conditions. This condition extends to the middle of the wind jet at 100 m. The upper half of the wind jet (100 to 250 m) caused a downward refraction region, as indicated by the increasing sound speed with height. This means that the sound will initially be refracted up away for the ground, causing rapid increase in the attenuation of sound with range until the acoustic wave reaches 100 m above ground level (AGL). Above this height, the acoustic wave will be refracted back toward the ground, forming an acoustic duct. This means that at a set range, the acoustic wave will reach the ground and reflect back up, resulting in a large decrease in the attenuation field. Looking to the east, the first 100 m are now downward refractive instead of upward. This means that the attenuation in this direction is not as great as it was to the north. The sound speed profile to the south also contains a downward refractive region over the first 100 m. Unlike the profile to the east, the downward refractive region to the south is not as thick as it is in the east. The impact of this is seen in the attenuation plots.

The attenuation plots were configured for a case of a helicopter flying 50 m AGL with a ground sensor 0.3 m from the ground. This simulates a battlefield acoustic array. The attenuation to the north of the helicopter (see Figure A-5) shows a rapid increase in the sound loss until the re-fracted wave returns and is reflected at 7 km. The rapid increase in the attenuation is attributable to the upward refractive layer in the sound speed profile mentioned before. Comparing Figure A-5 with A-6, it can be seen that the attenuation with range is much less in the east than the north. This is because of the absence of the upward refractive layer. The sound speed profile to the east shows a large downward refractive region extending 200 m in the atmosphere. The advantage of the downward refractive layer in the east assists in minimizing the attenuation initially, but the two graphs eventually show similar values for attenuation after the return wave arrives in Figure A-5. Finally, Figure A-7 shows the attenuation to the south. An interesting feature here is that initially, there is about the same amount of attenuation as in the east, but the attenuation is larger at greater

33
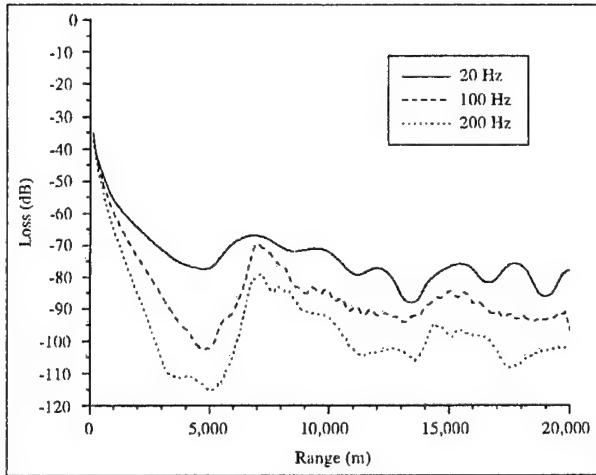
Figure A-5. Attenuation with range to the north of the target.
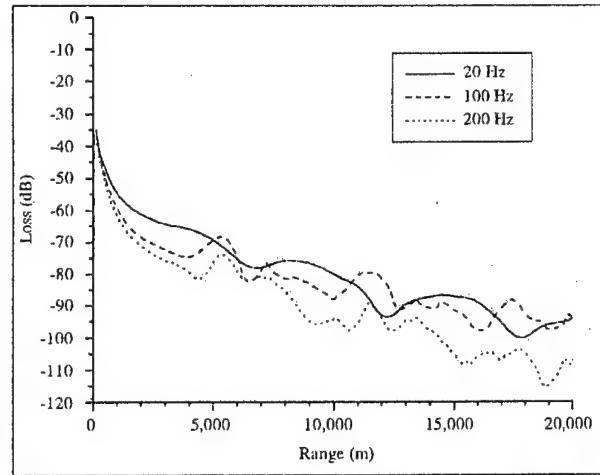
Figure A-6. Attenuation with range to the east of the target.
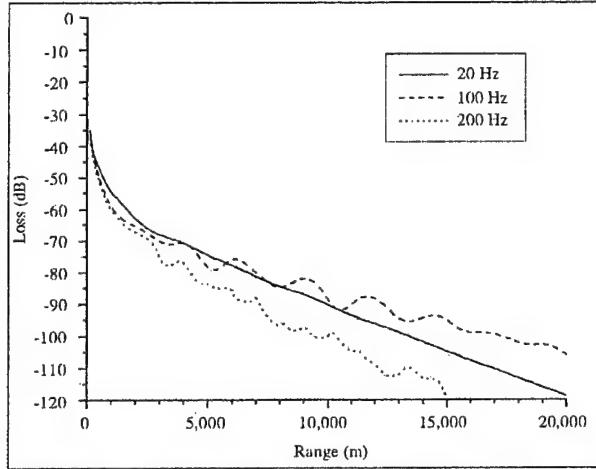
Figure A-7. Attenuation with range to the south of the target.

distance than the east. This is partially because of the height of the acoustic duct and the thickness of the region between the downward and upward refractive regions. The duct to the south is only 100 m thick, that is, only about three wavelengths at 20 Hz. Also, the thickness of the transition region is very small, so the diffraction of the refracted wave in this regions leads to the acoustic duct being "leaky". The term leaky refers to energy that is lost from the acoustic wave traveling inside a duct, thus decreasing the energy of the wave as it travels in the duct.

Figures A-8 through A-10 compare the attenuation of sound at 20, 100, and 200 Hz in the three directions. It can be seen in Figure A-8 that the acoustic wave initially loses the most energy but recovers it when the refracted wave returns from the downward refractive region. Also, the sound speed profile to the north contains the largest downward refractive region that traps the most acoustic energy within the duct. Figures A-9 and A-10 also illustrate these points for the 100- and 200-Hz signals. These frequencies show the effects of the upward refractive region better than the 20-Hz signal.

34
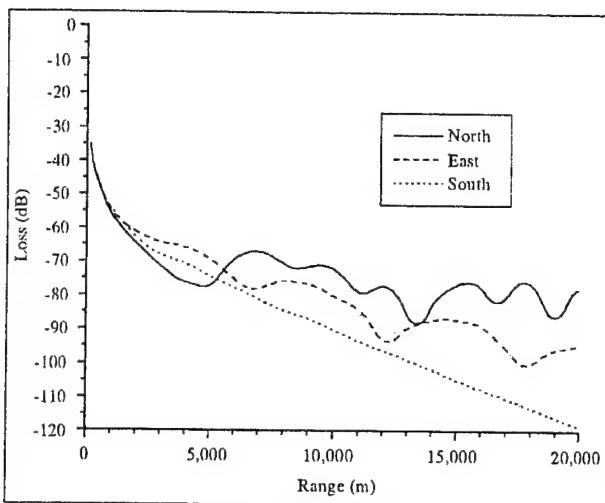
Figure A-8. Attenuation with range for the three directions at 20 Hz.
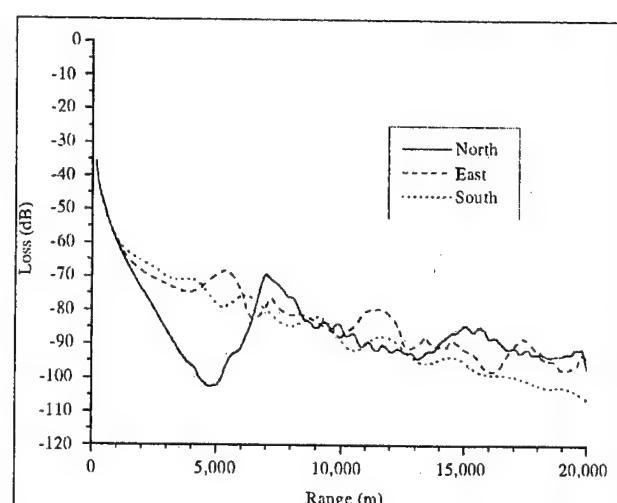

Figure A-9. Attenuation with range for the three directions at 100 Hz.
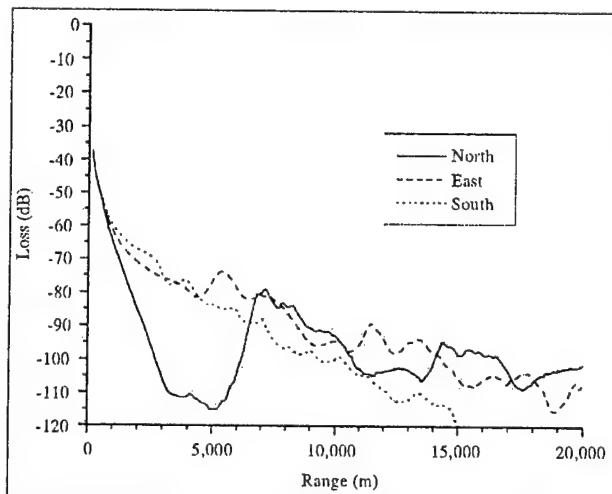
Figure A-10. Attenuation with range for the three directions at 200 Hz.

35

Appendix B. Meteorological Profile Builder Look-up Tables

Table B-1. IR emissivity

Ground Cover	ε
Fresh snow	0.99
Old snow	0.82
Dry sand	0.95
Wet sand	0.98
Dry peat	0.97
Wet peat	0.98
Soils	0.9 to 0.98
Asphalt	0.95
Concrete	0.71 to 0.9
Tar and gravel	0.92
Limestone gravel	0.92
Light sandstone rock	0.98
Desert	0.84 to 0.91
Grass lawn	0.97
Grass	0.90 to 0.95
Deciduous forests	0.95
Coniferous forests	0.97
Urban area (range)	0.85 to 0.95

Table B-2. Surface albedo

Surface	α	Surface	α
Snow and Ice		Urban (people influenced)	
Snow, fresh fallen	75 to 95	Road, black top	14
Snow, thawing	20 to 65	Road, stone	15
Snow, old	40 to 70	Road, dirt, wet	18
Snow, icy	75	Road, dirt, dry	35
Ice, grey	60	Road, clay, wet	20
Ice, white	75	Road, clay, dry &	
Ice, water covered	26	Road, asphalt, wet	10
Ice, light snow cover	31	Road, asphalt, dry	15
Ice, porous and melting	41	Parking lot, black top	8
Desert shrublands, snow covered	18 to 19	Concrete, new, white	37
Conifer forest, snow covered	59 to 67	Buildings	9
Mixed forest, 50 cm snow covered	20	Developed urban area (average)	15
Grasslands, snow covered	46 to 50	Roof, thatched, new	20
Crops, snow covered	18 to 19	Roof, thatched, old	15

Tundra, snow covered	59 to 67	Roof, tiled, dirty	8
Soil and Rocks		Crops, Natural Terrain, and Vegetation	
Soil, dark, wet	8	Fallow field, wet	5 to 7
Soil, dark, dry	13	Fallow field, dry	8 to 12
Soil, light, wet	10	Spring wheat	10 to 25
Soil, light, dry	18	Winter wheat	16 to 23
Dark organic soils	10	Rice paddy	12
Dark gray silt	12	Winter rye	18 to 23
Red soils	17	Forest, coniferous	5 to 15
Clay, wet	16	Forest, deciduous	10 to 20
Clay, dry	23	Grass, green	26
Clay loam, wet	19	Meadows, green	10 to 20
Clay loam, dry	13	Coniferous trees, dormant	12
Lime	45	Deciduous trees, dormant	12
Gypsum	55	Tall grass, dormant	13
Sand, white, wet	25	Mowed grass, dormant	19
Sand, white, dry	35	Tundra	15 to 20

Table B-3. Thermal properties of soils

Material	State	Soil Thermal Conductivity ($\times W\,m^{-1} \times K^{-1}$)	Soil Thermal Diffusivity ($\times m^2 \times h^{-1}$)
Sand	Dry	0.277	0.000900
Sand	Moist	2.0	0.002520
Sand	Saturated	2.2	0.002120
Quartz sand	Dry	0.264	0.000720
Quartz sand	8.3% moist	0.586	0.001188
Yolo silt loam	Dry	0.12	0.000450
Yolo silt loam	Moist	0.44	0.001860
Yolo silt loam	Saturated	0.848	0.001730
Sandy loam	Dry	0.23	0.000576
Sandy soil	Saturated	2.2	0.002660
Sandy clay	15% moist	0.925	0.001330
Clay soil	Dry	0.3	0.000549
Clay soil	Moist	1.47	0.003960
Clay soil	Saturated	1.58	0.001840
Clay pasture	—	2.76	0.004320
Calcareous soil	43% moist	0.712	0.000648
Soil (generic)	Very dry	0.167 to 0.345	0.00072 to 0.0011
Soil (generic)	Wet	1.26 to 3.35	0.000144 to 0.00036
Mud	—	0.84	0.000792
Peat soil	Dry	0.13	0.000540
Peat soil	Saturated	0.85	0.000432

Table B-4. Roughness length for different surfaces

Type of Surface	z_o (m)
Ice/Smooth mudflats	0.00001
Dry lake bed	0.00003
Tundra, snow covered	0.0001
Tundra, patchy snow	0.0003
Calm open sea	0.0001
Desert, smooth	0.0003
Farmland, snow covered	0.002
Bare soil, tilled	0.002 to 0.006
Prairie	0.01
Grass and trees, mixed	0.035
Brush, scrub growth, open	0.16
Brush, scrub growth, dense	0.25
Forested plateau, level topography	0.7 to 1.2
Forested plateau, rolling hills	1.25
Subtropical savanna, grass, few trees	0.31 to 0.41
Subtropical savanna, grass w/many shrubs	0.51 to 0.61
Coniferous forest	1.1
Residential, low density	1.1
City park	1.3
Urban, buildings, business district	1.75 to 3.20

REPORT DOCUMENTATION PAGE

Form Approved
OMB No. 0704-0188

1. AGENCY USE ONLY (Leave blank)	2. REPORT DATE January 2003	3. REPORT TYPE AND DATES COVERED Final, October 2000 to October 2001

4. TITLE AND SUBTITLE
User Manual for the Microsoft Window Edition of the Scanning Fast-Field Program (WSCAFFIP) Version 3.0

5. FUNDING NUMBERS
DA PR: AH71
PE: 62784A

6. AUTHOR(S)
John M. Noble

7. PERFORMING ORGANIZATION NAME(S) AND ADDRESS(ES)
U.S. Army Research Laboratory
Attn: AMSRL-CI-EP
2800 Powder Mill Road
Adelphi, MD 20783-1197

8. PERFORMING ORGANIZATION REPORT NUMBER
ARL-TR-2696

9. SPONSORING/MONITORING AGENCY NAME(S) AND ADDRESS(ES)
U.S. Army Research Laboratory
2800 Powder Mill Road
Adelphi, MD 20783-1197

10. SPONSORING/MONITORING AGENCY REPORT NUMBER

11. SUPPLEMENTARY NOTES
ARL PR: 2FEH26
AMS code: 622784H7111

12a. DISTRIBUTION/AVAILABILITY STATEMENT
Approved for public release; distribution unlimited.

12b. DISTRIBUTION CODE

13. ABSTRACT (Maximum 200 words)
The Scanning Fast-Field Program (SCAFFIP) is an atmospheric acoustic propagation model that incorporates many of the effects of the environment on the sound field such as geometrical spreading, refraction, diffraction, molecular absorption, and complex ground impedance. SCAFFIP provides the user with the attenuation levels with range and frequency for a given geometry and meteorological profile. The meteorological profile and geometry provides the model with the ability to calculate the sound speed profile. The geometry profile is required because of the angular dependence of the sound speed on the wind direction relative to the direction of propagation. This model works over a flat earth and non-turbulent atmosphere. Even with these restrictions, the model performs very well for many scenarios. The model contains a user-friendly interface that requires a minimum amount of information to run the model, yet there are flags that can be set to obtain more detailed information.

14. SUBJECT TERMS
Acoustics, Propagation, Atmosphere

15. NUMBER OF PAGES
46

16. PRICE CODE

17. SECURITY CLASSIFICATION OF REPORT Unclassified	18. SECURITY CLASSIFICATION OF THIS PAGE Unclassified	19. SECURITY CLASSIFICATION OF ABSTRACT Unclassified	20. LIMITATION OF ABSTRACT UL

NSN 7540-01-280-5500

Standard Form 298 (Rev. 2-89)
Prescribed by ANSI Std. Z39-18
298-102